Catalysis Science & Technology

Accepted Manuscript

ROYAL SOCIETY OF CHEMISTRY

www.rsc.org/catalysis

Journal Name Catalysis Science & Technology Dynamic Article Links ►

Cite this: DOI: 10.1039/c0xx00000x

www.rsc.org/xxxxxx

ARTICLE TYPE

Photoelectric Catalytic Reduction CO_2 to Methanol on the CdSeTe NSs/TiO_2 NTs

Peiqiang Li*, Jun Zhang, Huying Wang, Hua Jing, Jinfeng Xu, Xiaona Sui, Haitao Hu, Hongzong Yin*

Received (in XXX, XXX) Xth XXXXXXXXX 20XX, Accepted Xth XXXXXXXXX 20XX
DOI: 10.1039/b000000x

The CdSeTe nanosheets (CdSeTe NSs)/TiO_2 nanotubes (TiO_2 NTs) photoelectrocatalyst was obtained by the hydrothermal method, loading the CdSeTe NSs on TiO_2 NTs which was preparated by anodic oxidation method. The SEM and TEM results showed that CdSeTe was flaky structure with larger size of 300-400 nm and smaller size of about 100 nm, which distributed on the TiO_2 NTs surface uniformly. HRTEM and XRD characterization revealed that the CdSeTe NSs grew along the (100) and (002) orientations. Measured by UV-vis DRS and XPS, it narrowed the energy band gap of TiO_2 NTs from 3.20 eV to 1.48 eV by the introduction of CdSeTe NSs, of which conduction band and valence band located at -0.46 eV and 1.02 eV, respectively. In the photoelectrocatalytic reduction CO_2 process, the current density had a significant improvement after the CdSeTe NSs decorating, increasing from 0.31 mA cm^{-2} to 4.50 mA cm^{-2} at -0.8V. Methanol was the predominant photoelectrocatalytic reduction product identified by chromatography, and it reached 1166.77 μmol L^{-1} after 5 h. In addition, the mechanism of high efficiency photoelectrocatalytic reduction CO_2 to methanol was explained from the following aspects: energy band matching, high efficiency electron transmission and the stability of the catalyst.

*Corresponding author.Tel:86-0538-8249017 E-mail: chem_carbon@outlook.com; pqli@sdau.edu.cn

Cite this: DOI: 10.1039/c0xx00000x

www.rsc.org/xxxxxx

ARTICLE TYPE

1. Introduction

In recent years, energy crisis and global warming are two major problems that influence the human sustainable development. Serious environmental problems such as bad climates and rising sea levels are caused by the emission of CO_2 released from fossil fuels burning. Therefore, it has become a research hot point for constructing an environmental friendly non-fossil fuel type renewable energy system. To dates, there are many technologies relatively have been reported to convert CO_2 to alcohols, hydrocarbons with hydrogenation[1-9], in which the key issue is where the hydrogen coming from. In the traditional methods, heterogeneous and homogeneous catalytic hydrogenation processed at high temperature and pressure, and CO_2 catalytic copolymerization was still derived from fossil fuels[10-11], which had a little practical significance in the entire process. Inspiringly, the hydrogen from H_2O in photocatalytic (PC) reduction and electrocatalytic (EC) reduction CO_2 process has drawn much attention. Benefiting from renewable hydrogen generation by a clean and environmental friendly way, the above two methods are advanced processing technique with excellent catalytic performance for CO_2 reduction.

In 1979, it was reported for the first time that TiO_2 powder can achieve PC reduction of CO_2 to organics in aqueous solution by Inoue and Fujishima[12]. Since that, the TiO_2 system has been researched extensively and thoroughly, including morphology, crystalline phase and modification, etc[13-18]. Compared with TiO_2 nanoparticles and nanofilms, TiO_2 NTs have larger specific surface, more active sites and higher catalytic activity, getting more attentions[19]. Whereas, the wide energy band gap (E_g = 3.2 eV) of TiO_2 decides that it only can be excited by light with the wavelength shorter than 385 nm, which limits its practical application greatly[20]. As we all known, ultraviolet light (λ < 420 nm) accounts to less than 4 % in the whole solar spectrum, while the visible light is more than 45 %. In order to utilize the solar radiation efficiently, it is the fundamental way to develop the catalysts with stability, highly activity, low-cost and strong visible light response.

Great efforts have been made to solve the above mentioned problems. One of the most effective methods is to couple narrow energy band gap materials with TiO_2, which can obtain the new-typed promising catalysts with visible light response. Among the narrow energy band gap materials, Ⅱ-Ⅵ semiconductors CdX (X = S, Se, Te) with an energy band gap of 1.43-2.53 eV[21-22] have strong absorption for visible light and higher photoelectric conversion efficiency. CdS has a wider band gap of 2.53 eV[21] and can only be excited by the irradiation wavelength shorter than 517 nm. Though the absorption wavelength can be extended to 890 nm from 517 nm by means of squash sintering, coating, spray pyrolysis and spectral sensitization with RuS_2, the photoelectric conversion efficiency is still very low relatively. The research focus turns to CdSe, CdTe with narrower band gap (1.74–1.43 eV) [22]. The photoelectric conversion efficiency of CdSe reached 3.6% when the photoanode was photoelectrochemically etched[23]. Soon afterwards, the researchers prepared $CdSe_xTe_{1-x}$ films through using Te instead of a part of Se, its spectral response of $CdSe_xTe_{1-x}$ film depends on 'x' value, and the photoelectric conversion efficiency could reach up to 8% when x = 0.65[23]. Apparently, $CdSe_xTe_{1-x}$ is a more promising photocatalyst than CdS and CdTe because of its better photoelectric property and stability.

However, as a kind of narrow energy band gap material, $CdSe_xTe_{1-x}$ may be oxidized easily by the photo-generated holes itself, which resulted in inactivation[24]. To the best of our knowledge, there are two main methods to avoid photocorrosion. The most representative one is to synthesize core-shell structure material[25-28], which can solve the photocorrosion problem to a great extent for the protective layers existing. The other one is to separate and transmit the photogenerated electron-hole in time, which can solve the photocorrosion problem fundamentally. Since the flaky structure has the excellent capability of seperation and transmission for the photogenerated electron-hole, we hope to design a photocatalyst with the special flaky structure. The ultimate goal is to design a photoelectrocatalytic (PEC) material, which not only has narrow energy band gap, but also possess excellent stability.

Our research group aimed to gain a structure of CdSeTe/TiO_2 similar to solar panels which could absorb sunlight well on the roof: orderly CdSeTe with flaky structure prepared by hydrothermal method equivalent to the solar panels, the TiO_2 NTs obtained by anodic oxidation method similar to the roof. In experiments, it was found that the as-prepared CdSeTe NSs/TiO_2 NTs with particular structure could absorb and utilize visible light efficiently indeed. Furthermore, the CdSeTe NSs/TiO_2 NTs simultaneously had excellent PC and EC performance on CO_2 reduction. To the best of our knowledge, it might be the first time to prepare the CdSeTe NSs/TiO_2 NTs with the flaky structure, and perhaps it was also the first time that the structure to be used in PEC reduction of CO_2. We hope that the research could provide not only a new idea to design the composite catalyst on PEC reduction of CO_2, but also great guidance and theory significance for PEC reduction of CO_2

2. Experimental Methods

TiO_2 NTs were obtained according to previous reports[29]. All chemical reagents were analytical grade. Typically, cadmium chloride solution ($CdCl_2$, 40 mmol L^{-1}), trisodium citrate dihydrate ($C_6H_5Na_3O_7{\cdot}2H_2O$, 100 mg), sodium selenite (Na_2SeO_3, 10 mmol L^{-1}) and sodium tellurite (Na_2TeO_3, 10 mmol L^{-1}) were added into a conical flask and diluted into 50 mL with ultrapure water, and then mercaptosuccinic acid (MSA, 60 mg), sodium borohydride ($NaBH_4$, 45 mg) were added in sequence under continuous magnetic stirring. The solution was placed in Teflon-lined stainless reactor with TiO_2 NTs at 120 ^oC for 2 h. TiO_2 NTs

modified by CdSeTe were dried at 80 °C, and then treated at 500 °C for 2 h under nitrogen atmosphere with heating and cooling rate of 2 °C min^{-1}. Scheme 1 shows the preparation process of the catalyst.

The surface morphologies of the as-prepared samples were characterized by scanning electron microscopy (SEM, Philips XL30 FEG) with accelerated voltage of 20 kV and high resolution transmission electron microscopy (HRTEM, FEI/Philips Techal 12 BioTWIN). The crystalline structures were characterized by X-ray diffraction (XRD, Rigaku D/MAX-rA, Japan) using Cu Kα radiation (λ = 15.4184 nm) in the range of 2θ = 20-70 ° with scan rate of 4 ° min^{-1}. Surface compositions were detected by X-ray photoelectron spectroscopy (XPS, ESCALAB 250) with a monochromated X-ray source (Al Kα $h\nu$ = 1486.6 eV). The UV-visible diffuse reflection spectrum (UV-visible DRS) was to measure the photochemical properties (Beijing Purkinje General Instrument Co., Ltd). The electrochemical properties were measured by CHI660D electrochemical workstation (Shanghai Chenhua Instrument Co., Ltd).

The PEC properties were measured by CHI660D electrochemical workstation with a traditional three electrodes system. Saturated calomel electrode (SCE) was used as reference electrode, platinum wire as counter electrode, CdSeTe NSs/TiO_2 NTs or TiO_2 NTs as working electrode, respectively. 500W Xenon lamp (Solar-500, NBeT Group Corp.) with a filter ($\lambda \geq$ 420 nm, 100 mW cm^{-2}) served as the visible light. Linear sweep voltammetry (LSV) was measured in 0.1 mol L^{-1} $KHCO_3$ with a scan rate of 50 mV s^{-1}. N_2 or CO_2 were bubbled into $KHCO_3$ solution at the rate of 40 sccm for 20 min before experiment.

PEC reduction CO_2 experiments were conducted in a double cells reactor with circulating water at the constant temperature of 25 °C. CdSeTe NSs/TiO_2 NTs or TiO_2 NTs, platinum wire and SCE was used as working electrode, counter electrode and reference electrode, respectively. Electrode area was 2×2 cm^2, and electrode interval was 1.0 cm. The flow rate of CO_2 was 40 mL min^{-1} during the whole experiment. 500W Xenon lamp ($\lambda \geq$ 420 nm, 100 mW cm^{-2}) served as the source of visible light. The intermediates and productions were detected by gas chromatography (6890-N, Agilent) with column (2 m, inner diameter 3 mm, Parapok Q, 80-100) and flame ionization detector. The column temperature was kept at 100 °C while the detector temperature was at 150 °C. High purity N_2 worked as carrier gas with a flow rate of 30 sccm.

3. Results and Discussion.

Fig. 1a depicted the SEM image of CdSeTe NSs/TiO_2 NTs. It could be seen that the CdSeTe grew to be flaky structure with different shapes, such as pentagons, quadrilaterals and other polygons, etc. Their sizes were different from 100 nm to 350 nm. The insert chart in the left corner indicated the TiO_2 NTs morphology was ordered arrays before loading CdSeTe NSs, with diameter of 90-100 nm. The flakes grew compactly on the surface of TiO_2 NTs. None the less, TiO_2 NTs could be clearly seen from the gap of the flakes. In addition, we could clearly find the single nanosheet with length of 355 nm and width of 291 nm from the HRTEM of CdSeTe NSs (Fig. 1b). HRTEM in Fig. 1c was the further enlarged image of CdSeTe NSs, showing the strip fingerprint structure of the nanosheet. The strip fingerprint structure revealed that CdSeTe NSs grew along two orientations with the lattice spaces of 0.39 nm and 0.36 nm, respectively. Compared with the standard lattice constant, it could be concluded that CdSeTe grew along the (100) and (002) orientation crystal plane. Thus, we could infer that CdSeTe prepared on the TiO_2 NTs was a two-dimensional orderly flaky structure. The flaky structure was just like polysilicon solar panels, which were placed on the roof surface (TiO_2 NTs). The flaky CdSeTe with a large specific surface and the TiO_2 with tubulose structure, might be favorable to the light absorption and the separation of photo-generated electron-hole[30]. Furthermore the specific structure might be propitious to improve the photoelectric conversion efficiency.

Fig. 2 showed the XRD of the sample scraped from the as prepared material surface. The strong and sharp diffraction peaks indicated that CdSeTe NSs owned excellent crystallization. The major strong characteristic peaks of CdSeTe NSs were at 23.02 °, 24.28 °, 33.26 °, which corresponded to the crystal planes of (100), (002) and (102), respectively. And the lattice parameters were calculated as a = 4.4613 Å and c = 7.2452 Å, which was consistent with JCPDS card (No. 41-1325). It indicated that the prepared material exactly was CdSeTe. The CdSeTe NSs grew along (100) and (002) orientations which was in keeping with HRTEM conclusion very well. And the conclusion was once again proved the two-dimensional orderly flaky structure. The (102) crystal panel might be interpreted as the crystal panel caused by the interface of CdSeTe NSs and TiO_2 NTs, which had not been demonstrated in this study.

About the visible light absorption of as prepared materials, it could be seen that the light absorption of CdSeTe NSs/TiO_2 was stronger than that of TiO_2 NTs (Fig. 3a). The result proved that the optical absorption of the material was enhanced greatly by the introduction of CdSeTe NSs. The energy band gap of CdSeTe NSs/TiO_2 NTs was 1.48eV, which is estimated by a linear fit to the experimental $(\alpha h\nu)^2$ versus hν plot (Fig. 3b). It is narrower than the previous report (1.98 - 2.17 eV) [31]. It indicated that the materials can be excited by the light with low energy ($\lambda \leq$ 838 nm), which improved the utilization of light obviously.

The XPS spectrum was measured to obtain the chemical components and the oxidation states of the materials. The wide scan XPS spectrum (Fig. 4a) revealed the predominant presence of C, O, Ti, Cd, Se and Te elements. Among the elements, O, Ti, Cd, Se and Te elements were from the as-prepared composite and the C element originated from the XPS instrument itself. No other heteroelement was detected. Higher resolution spectrums of Ti 2p, Se 3d, Te 3d and Cd 3d were shown in Fig. 4b, 4c, 4d and 4e: Ti ($2p_{3/2}$ and $3d_{1/2}$) at 458.4 and 463.5 eV, Se 3d at 53.1 eV, Te ($3d_{5/2}$ and $3d_{3/2}$) at 575.7 eV and 583 eV, and Cd($3d_{5/2}$ and $3d_{3/2}$) at 405.1 eV and 411.8 eV, respectively. All these data are consistent with the standard data values and indicate that CdSeTe NSs/TiO_2 NTs are comprised of Ti^{4+}, Cd^{2+}, Se^{2-}, and Te^{2-}.

Fig. 4f showed the valence band photoemission spectrum of CdSeTe NSs/TiO_2 NTs and its Gaussian fit. There were two distinguished peaks with centers at 5.38 eV and 10.84 eV in the photoemission spectrum. These peaks were attributed to the electron emission from π (nonbonding) and s (bonding) O 2p orbital, respectively. The location of the valence band maximum (VBM) was determined directly from the electron emission

spectrum by methods of a linear extrapolation of the onset of the valence band emission[32-33]. The VBM was found to be located at about 1.02 eV. From the calculated energy band gap of 1.48 eV by UV-vis DRS, we could deduce that the conduction band minimum (CBM) was located at -0.46 eV.

The Linear sweep voltammery (LSV) was measured in the 0.1 mol L^{-1} $KHCO_3$ solution (Fig. 5). The increase of current density attributed to two main factors: one was the reduction of H_2O to H_2, and the other was the reduction of CO_2. Before the hydrogen evolution reaction, CO_2 reduction was the main factor. When the hydrogen evolution reaction takes place, hydrogen evolution and CO_2 reduction become competitive reactions leading to the current density significant increase. It can be seen that the current density increased obviously on the TiO_2 NTs (curves e > f) when N_2 was replaced by CO_2, which indicated TiO_2 NTs had EC effect on reducing CO_2. But there was few PC effect under illumination, because the current density had almost no increase (curves e and d). After modifying CdSeTe NSs, the current density was much larger than that of TiO_2 NTs in the CO_2 saturated solution(curve b > e), it indicated that the EC reduction for CO_2 was enhanced by the introduction of CdSeTe NSs. Furthermore, after introducing illumination, the current density had further increased (curve a > b). It indicated that CdSeTe NSs/TiO_2 NTs had excellent PC performance as well as outstanding EC performance.

Fig. 6a was the products analysis of CdSeTe NSs/TiO_2 NTs PEC reduction of CO_2 under different potentials. Methanol and methane were detected, and the detailed data were listed in the Table 1. It can be seen clearly that methanol was the predominant product, and its yield increased firstly and then decreased with the potential varied from -0.6 V to -1.2 V, and it reached the peak at -0.8 V. We explained the phenomenon as followed: in the range of -0.6 V ~ -0.8 V, CO_2 reduction was the main reaction, there was no hydrogen evolution reaction. With the potential towards more negative, EC CO_2 reduction strengthened gradually. When the potential was -0.8 V, PEC CO_2 reduction achieved optimum and the yield of methanol reached a peak. When the potential was more negative than -0.8 V, hydrogen evolution reaction began to take place (Fig. 5, the curve a). Therefore, the CO_2 reduction and hydrogen evolution reactions were competitive, which decreased the catalytic reduction efficiency of CO_2 and the methanol yield. Consequently, the yield of methanol reached its maximum at -0.8 V, and the Faradaic Efficiency[34] also reached a maximum 87.95%.

$$\text{Faradaic efficiency} = \frac{\text{moles product} \times \text{number of electrons needed for conversion}}{\text{moles of electrons passed}} \quad \ldots\ldots\ldots\ldots\ldots (1)$$

We ascribed the reason of CdSeTe NSs/TiO_2 NTs highly efficiently reducing CO_2 to methanol for two main aspects: one was the material structure resulting in its high efficiency. The flaky structure of the as-prepared material had excellent electronic transmission performance. It could be seen from Fig. 7 that the EIS of CdSeTe NSs/TiO_2 NTs (2.21 kΩ) was much smaller than that of the TiO_2 NTs (31.19 kΩ). It proved that the introduction of CdSeTe NSs decreased the resistance of the substrate and further improved the electron transfer, which can provide enough electrons for the CO_2 reduction. The other was the suitable energy band matching of the catalyst. The band gap of CdSeTe NSs/TiO_2 NTs was 1.48 eV, so the catalyst could be excited by the light shorter than 838 nm, and it had better performance in light absorption and utilization (Fig. 3, red line). In addition, its conduction band loaded at -0.46 eV, which was lower than the reduction potential of CO_2/CH_3OH (-0.38 V). This indicated that the catalyst possessed enough reductive ability to reduce CO_2 to methanol. At the same time its valence band loaded at 1.02 eV, which was higher than the oxidation potential of H_2O/O_2 (0.82 V). It indicated that the catalysis possessed enough oxidative ability for H_2O splitting to provide H^+ for CO_2 reduction ($CO_2+6e^-+6H^+=CH_3OH+H_2O$) (Scheme 2). As the two factors above, CdSeTe NSs/TiO_2 NTs can reduce CO_2 to methanol efficiently.

At the same time, CdSeTe NSs/TiO_2 NTs had outstanding photoelectric stability. Fig. 6b showed that the curve had good linear relation between methanol concentration logarithm and time. It fitted the first order reaction model of thermodynamics, the reaction rate constant was 2.72×10^{-3} min^{-1}, which indicated fully the as-prepared catalyst had good photoelectric stability. We thought the stability was attributed to excellent electronic transmission performance decided by the flaky structure and efficient PEC performance decided by energy band matching. This conclusion further explained the reason of efficiently generating methanol on CdSeTe NSs/TiO_2 NTs.

4. Conclusions

In this paper, CdSeTe NSs were assembled to the TiO_2 NTs by hydrothermal method to obtain the target catalyst CdSeTe NSs/TiO_2 NTs. The catalyst with energy band gap 1.48eV could be excited by the visible light with wavelength less than 838 nm. Meanwhile, it has excellent PEC performance. After applying CdSeTe NSs/TiO_2 NTs to PEC reduction CO_2, we found that it had high efficiently catalytic performance for CO_2 reduction, and the major product was methanol. The methanol generation efficiency was the highest at -0.8 V, and the methanol concentration reached 1166.77 μmol L^{-1} after 5 h. At last, the high efficiency mechanism of CdSeTe NSs/TiO_2 NTs PEC reducing CO_2 to methanol was hypothesized. The high efficiency of the as-prepared catalyst was explained from the following three aspects: excellent electronic transmission performance decided by the flaky structure, efficient PEC performance decided by energy band matching, and the photoelectric stability of the catalyst.

5. Acknowledgements

This research was supported by the National Natural Science Foundation of China (Grant No. 21203114), Key Projects in the National Science & Technology Pillar Program during the Twelfth Five-year Plan Period (Grant No. 2011BAD11B01), and Promotive Research Fund for Excellent Young and Middle-aged Scientists of Shandong Province (Grant No. BS2012NJ008). We are grateful to the foundation supported by Shandong Jingbo Holdings Corporation.

Notes and References

College of Chemistry and Material Science, Shandong Agricultural University, 271018, People's Republic of China Tel:86-0538-8249017

E-mail: chem_carbon@outlook.com; pqli@sdau.edu.cn

1 E.E. Barton, D.M. Rampulla, A.B. Bocarsly, *J. Am. Chem. Soc.*, 2008, **130**, 6342.
2 E. Balaraman, C. Gunanathan, J. Zhang, L.J.W. Shimon, D. Milstein, *Nature Chem.*, 2011, **3**, 609.
3 O.K. Varghese, M. Paulose, T.J. LaTempa, C.A. Grimes, *Nano Lett.*, 2009, **9**, 731.
4 H. Takeda, K. Koike, H. Inoue, O. Ishitani, *J. Am. Chem. Soc*., 2008, **130**, 2023.
5 G. Ménard, D.W. Stephan, *J. Am. Chem. Soc.*, 2010, **132**, 1796.
6 M.R. Dubois, D.L. Dubois, *Acc. Chem. Res.*, 2009, **42**, 1974.
7 Y.Y. Liu, B.B. Huang, Y. Dai, X.Y. Zhang, X.Y. Qin, M.H. Jiang, M.H. Whangbo, *Acc. Chem. Res.*, 2009, **11**, 210.
8 G.H. Liu, N. Hoivik, K.Y. Wang, H. Jakobsen, *Sol. Energy Mater. Sol. Cells*, 2012, **105**, 53.
9 J. Mao, K. Lia, T.Y. Peng, *Catal. Sci. Technol.* , 2013, **3**, 2481-2498
10 X.M. Guo, D.S. Mao, S. Wang, G.H. Wu, G.Z. Lu, *Acc. Chem. Res.*, 2009, **10**, 1661.
11 M.E. Berndt, D.E. Allen, W.E. Seyfried, Jr, *Geology*, 1996, **24**, 351.
12 I. Tooru, F. Akira, K. Satoshi, H. Kenichi, *Nature*, 1979, **277**, 637.
13 P. Panagiotopoulou, D.I Kondarides, *Catal.*, 2004, **6**, 327.
14 K. Kočí, K. Matějů, L. Obalová, S. Krejčíková, Z. Lacný, D. Plachá, L. Čapek, A. Hospodková, O. Šolcová, *Appl. Catal., B: Environ.*, 2010, **96**, 239.
15 J.Y. Shi, J. Chen, Z.C. Feng, T. Chen, Y.X. Lian, X.L. Wang, C. Li, *J. Phys. Chem. C.*, 2007, **111**, 693.
16 A. Naldoni, M. Allieta, S. Santangelo, M. Marelli, F. Fabbri,S. Cappelli, C.L. Bianchi, R. Psaro, V.D. Santo, *J. Am. Chem. Soc.*, 2012, **134**, 7600.
17 V.M. Aroutiounian, V.M. Arakelyan, G.E. Shahnazaryan, *Sol. Energy Mater. Sol. Cells*, 1995, **89**, 153.
18 M. Hussain, R. Ceccarelli, D.L. Marchisio, D. Fino, N. Russo, F. Geobaldo, *Chem. Eng. J.*, 2010, **157**, 45.
19 A.E.R. Mohamed, S. Rohani, *Energy Environ. Sci*., 2011, **4**, 1065.
20 Z.H. Zhang, M. Faruk Hossain, T. Takahashi, *Appl. Catal., B: Environ.*, 2010, **95**, 423.
21 L.A. Swafford, L.A. Weigand, M.J. Bowers, J.R. McBride, J.L. Rapaport, T.L. Watt, S.K. Dixit, L.C. Feldman, S.J. Rosenthal, *Am. Chem. Soc.*, 2006, **128**, 12299.
22 S.S. Lo, T. Mirkovic, C.H. Chuang, C. Burda, G.D. Scholes, *Adv. Mater.*, 2011, **23**, 180.
23 R. Tenne, G. Hodes, *Appl. Phys. Lett.*, 1980, **37**, 428.
24 A. Henglein, *J. Phys. Chem.*, 1982, **86**, 2291.
25 Y. Kobayashi, T. Nozawa, T. Nakagawa, K. Gonda, M. Takeda, N. Ohuchi, A. Kasuya, *J Sol-Gel Sci Technol.*, 2010, **55**, 79.
26 G.X. Liang, L.L. Li, H.Y. Liu, J.R. Zhang, C. Burda, J.J. Zhu, *Chem. Commun.*, 2010, **46**, 2974.
27 G. Beaune, S. Taman, A. Bernardin, P. Bayle-Guillemaud, D. Fenel, G. Schoehn, F. Vinet, P. Reiss, I. Texier, *Chem. Phys. Chem.*, 2011, **12**, 2247.
28 Y.Y. Shen, L.L. Li, Q. Lu, J. Ji, R. Fei, J.R. Zhang, E. S. Abdel-Halim, J.J. Zhu, *Chem. Commun.*, 2012 , **48**, 2222.
29 P.Q. Li, G.H. Zhao, X. Cui, Y.G. Zhang, Y.T. Tang, *J. Phys. Chem. C.*, 2009, **113**, 2375.
30 D.J. Xue, J.H. Tan, J.S. Hu, W.P. Hu, Y.G. Guo, L.J. Wan, *Adv. Mater.*, 2012, **24**, 4528.
31 V. Lesnyak, A. Dubavik, A. Plotnikov, N. Gaponik, A. Eychmüller, *J. Phys. Chem. C.*, 2008,**112**, 15253.
32 T. Nikolay, L. Larina, O. Shevaleevskiy, B. Tae Ahn, *Energy Environ. Sci*, 2011, **4**, 1480.
33 D.K. Bora, A. Braun, R. Erni, G. Fortunato, T. Graule, E.C. Constable, *Chem. Mater*, 2011, **23**, 2051.
34 B. Kumar, M. Llorente, J. Froehlich, T. Dang, A. Sathrum, C. P. Kubiak, *Annu. Rev. Phys. Chem.,* 2012, **63**, 541.

Graphical Abstract

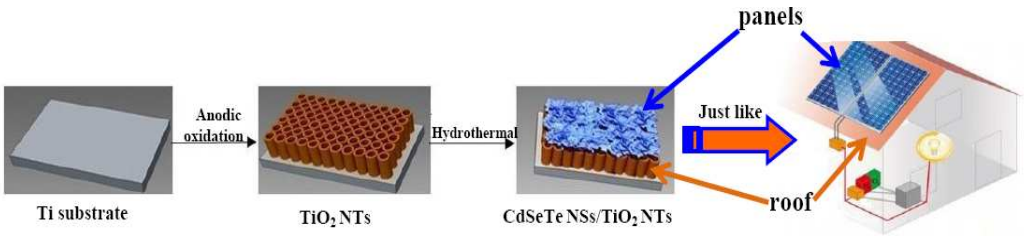

Scheme of CdSeTe NSs/TiO_2 NTs preparation

Prepare orderly CdSeTe with flaky structure (similar the solar panels), and then assemble CdSeTe nanosheets (CdSeTe NSs) onto the TiO_2 NTs (the TiO_2 NTs equivalent the roof).